1776 *Chem. Mater.* **2010,** *22,* 1776–1781
DOI:10.1021/cm9032513

CHEMISTRY OF MATERIALS
Article

Self-Assembly and Enhanced Magnetic Properties of Three-Dimensional Superlattice Structures Composed of Cube-Shaped EuS Nanocrystals

Atsushi Tanaka,[†] Hironari Kamikubo,[†] Yoshihiro Doi,[‡] Yukio Hinatsu,[‡] Mikio Kataoka,[†] Tsuyoshi Kawai,*[,†] and Yasuchika Hasegawa*[,†]

[†]*Graduate School of Materials Science, Nara Institute of Science and Technology, 8916-5 Takayama-cho, Ikoma, Nara 630-0192, Japan, and* [‡]*Graduate School of Science, Hokkaido University, North 10 west 8, Sapporo, Kokkaido 060-0810, Japan*

Received October 23, 2009. Revised Manuscript Received January 6, 2010

Superlattice structures (SLSs) assembled with cube-shaped EuS nanocrystals (NCs) and their remarkable magnetic properties are reported. The cube-shaped EuS NCs are prepared by the thermal reduction of single source precursor, tetra(diethyldithiocarbamate) europium complex with oleylamine as a surface modified regent. The fine structures of the three-dimensional (3D) SLSs assembled with EuS NCs are characterized by TEM, small-angle XRD, and electron transmission tomographic analysis. Magnetic measurements of the SLSs on polymer films with SQUID show that the coercive field of the SLSs assembled with cube-shaped EuS NCs are twice larger than those of cube-shaped EuS NCs powder. The enhanced magnetic properties are attributed to magnetic dipole interaction between cube-shaped EuS NCs in SLS structures.

Introduction

For the past few decades, considerable attention has been focused on the preparation and properties of magnetic semiconductors from the view points of fundamental condensed matter science and also of practical application for spintronics and magneto-optic devices.[1] In order to manipulate their magnetic and magneto-optic properties, various types of structured magnetic materials have been prepared.[2−5] Preparation of semiconductor nanocrystals (NCs) with magnetic dopants has also been studied, and stochastic control for a number of magnetic dopants in II−VI or III−V semiconductor NCs has been investigated.[6] However, the characteristic magnetic properties of the semiconductor NCs may not have been studied extensively, because there are few classes of materials that exhibit both intrinsic magnetic and semiconducting properties.[7] One of the most important series of intrinsic magnetic semiconductors is europium chalcogenides, EuX (X = O, S, Se, and Te).[8] The EuX have been intensely studied in the 1970s and continue to be of both theoretical and experimental interest. The EuX semiconductors are characterized by narrow 4f orbitals that exist as degenerate levels between the conduction band (5d orbitals of Eu(II)) and the valence band (p orbitals of O^{2-}, S^{2-}, Se^{2-}, or Te^{2-}).[8] The 4f-5d electronic transition and spin configuration of europium(II) chalcogenides lead to large Faraday and Kerr effects,[9] which make them the promising candidates as active materials in magneto-optic devices.

Recently, NCs of EuO, EuS, and EuSe have been synthesized, and their resulting magnetic and magneto-optical properties have been explored.[10] Among them, EuS NCs have been focused as promising materials because of their ferromagnetic properties with Curie temperature, T_C of 16.6 K, and characteristic Faraday

*Corresponding author. Tel./Fax: +81 743 6171. E-mail: hasegawa@ms.naist.jp (Y.H.), tkawai@ms.naist.jp (T.K.).

(1) Furdyna, J. K. *J. Appl. Phys.* **1988**, *64*, R29–R64.
(2) Gaj, J. A.; Ginter, J.; Galazka, R. R. *Physica Status Solidi B* **1978**, *89*, 655–662.
(3) Ohno, H.; Shen, A.; Matsukura, F.; Oiwa, A.; Endo, A.; Katsumoto, S.; Iye, Y. *Appl. Phys. Lett.* **1996**, *69*, 363–365.
(4) Ohno, Y.; Young, D. K.; Beschten, B.; Matsukura, F.; Ohno, H.; Awschalom, D. D. *Nature* **1999**, *402*, 790–792.
(5) Jungwirth, T.; Atkinson, W. A.; Lee, B. H.; MacDonald, A. H. *Phys. Rev. B* **1999**, *59*, 9818–9821.
(6) Wang, Y.; Herron, N.; Moller, K.; Bein, T. *Solid State Commun.* **1991**, *77*, 33–38.
(7) (a) Norris, D. J.; Yao, N.; Charnock, F. T.; Kennedy, T. A. *Nano Lett.* **2001**, *1*, 3–7. (b) Jun, Y. W.; Jung, Y. Y.; Cheon, J. *J. Am. Chem. Soc.* **2002**, *124*, 615–619. (c) Schwartz, D. A.; Norberg, N. S.; Nguyen, Q. P.; Parker, J. M.; Gamelin, D. R. *J. Am. Chem. Soc.* **2003**, *125*, 13205–13218. (d) Stowell, C. A.; Wiacek, R. J.; Saunders, A. E.; Korgel, B. A. *Nano Lett.* **2003**, *3*, 1441. (e) Norberg, N. S.; Kittilstved, K. R.; Amonette, J. E.; Kukkadapu, R. K.; Schwartz, D. A.; Gamelin, D. R. *J. Am. Chem. Soc.* **2004**, *126*, 9387–9398. (f) Erwin, S. C.; Zu, L.; Haftel, M. I.; Efros, A. L.; Kennedy, T. A.; Norris, D. J. *Nature* **2005**, *436*, 91–94. (g) Beaulac, R.; Archer, P. I.; Liu, X.; Lee, S.; Salley, G. M.; Dobrowolska, M.; Furdyna, J. K.; Gamelin, D. R. *Nano Lett.* **2008**, *8*, 1197–1201.
(8) Wachter, P. *Handbook on the Physics and Chemistry of Rare Earth*, 2nd ed.; CRC Critical Reviews in Solid State Science; North-Holland Publishing Company: 1979; pp 189−241.
(9) Suits, J. C.; Argyle, B. E.; Freiser, M. J. *J. Appl. Phys.* **1966**, *37*, 1391–1397.
(10) (a) Hasegawa, Y.; Thongchant, S.; Wada, Y.; Tanaka, H.; Kawai, T.; Sakata, T.; Mori, H.; Yanagida, S. *Angew. Chem., Int. Ed.* **2002**, *41*, 2073–2075. (b) Thongchant, S.; Hasegawa, Y.; Wada, Y.; Yanagida, S. *J. Phys. Chem. B* **2003**, *107*, 2193–2196. (c) Hasegawa, Y.; Afzaal, M. A.; O'Brien, P.; Wada, Y.; Yanagida, S. *Chem. Commun.* **2005**, 242–243. (d) Kataoka, T.; Tsukahara, Y.; Hasegawa, Y.; Wada, Y. *Chem. Commun.* **2005**, 6038–6040. (e) Hasegawa, Y.; Okada, Y.; Kataoka, T.; Sakata, T.; Mori, H.; Wada, Y. *J. Phys. Chem. B* **2006**, *110*, 9008–9011. (f) Hasegawa, Y.; Adachi, T.; Tanaka, A.; Afzaal, M.; O'Brien, P.; Doi, T.; Hinatsu, Y.; Fujita, K.; Tanaka, K.; Kawai, T. *J. Am. Chem. Soc.* **2008**, *130*, 5710–5715.

Published on Web 01/28/2010

effects in visible region.[10,11] The energy level of the conduction band constructed from 5d orbitals should be affected by the size of NCs as like those of other semiconductor NCs. The effective mass of electron in EuS is estimated at 0.3−1.1 by previous reports.[12] Therefore, the electron Bohr radius is calculated to be 0.7−2.3 nm. EuS NCs with smaller size (diameter ∼ 5 nm) could be thus affected by the quantum size effect, to some extent. Accordingly, the energy gap between the 4f orbitals and the conduction band can be manipulated by controlling the size of EuS NCs with the quantum size effect, and their magneto-optic properties are markedly enhanced in the EuS NCs because of their quantum-confinement effects on the electronic excited states with enhanced spin−orbital interaction.[10d] The magneto-optical properties of EuS NCs depend on not only their size but also their shape and surface environments.[10,11] In order to enhance their magnetic properties, we here attempted to construct superlattice structures (SLSs) by building up NCs with self-assembling procedure. Preparation of SLSs composed of semiconductor NCs with magnetic properties have never been reported because of difficulty in controlling the amount of magnetic dopants, size, and shape of the NCs precisely. According to magnetic materials, enhanced magnetic properties of SLSs of FePt, γ-Fe_2O_3, Fe, and ε-Co NCs have been recently studied.[13] Chaudret et al. have reported on electron holography approach to investigate the magnetic properties of cube-shaped magnetic Fe NCs.[14] Their enhanced magnetic properties are based on their magnetic dipole interaction between the NCs. Characteristic properties of SLSs assembled with II−VI or III−V semiconductor NCs have also been reported.[15] In particular, Urban et al. have reported that the SLSs composed of semiconductor NCs showed remarkable electronic properties because of characteristic exciton coupling between the NCs.[16] Regarding the characteristic magnetic and electronic properties of SLSs, well-organized SLSs of magnetic semiconductor cube-shaped EuS NCs are thus expected to exhibit enhanced spin polarization and magnetic properties.

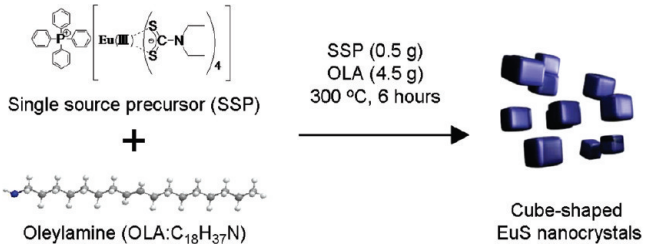

Figure 1. Reaction schemes of cube-shaped EuS NCs.

Here, we report on self-assemblies and their specific magnetic properties of three-dimensional (3D) SLSs composed of EuS NCs with cubic shapes. The EuS NCs are prepared under precise control of the reaction time and temperature of the thermal decomposition of single source precursor, tetraphenyl phosphonium tetra (diethyldithiocarbamate)-europium complex, $(PPh_4)[Eu(S_2CNEt_2)_4]$ with oleylamine (OLA) as a surface modified regent (Figure 1). We have attempted to prepare 3D SLSs composed of cube-shaped EuS NCs on TEM grids and polymer films. The fine structures of the 3D SLSs were characterized by TEM and small-angle XRD measurements and TEM including 3D tomographic observation. We also measured these magnetic properties of the SLSs on polymer films and observed that coercive fields of SLSs on the films were two times larger than those of EuS NCs powder. In the present study, self-assmbling formation and enhanced magnetic properties of SLSs of EuS NCs are demonstrated for the first time.

Experimental Section

1. Materials. Europium(III) chloride hexahydrate ($EuCl_3 \cdot 6H_2O$) was purchased from Kanto Chemical Co. Inc. Sodium *N,N*-diethyldithiocarbamate trihydrate ($Na(S_2CNEt_2) \cdot 3H_2O$) and toluene were purchased from Nacalai Tesque. Tetraphenylphosphonium bromide ($BrPPh_4$) and acetonitrile-d_3 (CD_3CN) were purchased from Wako Pure Chemical Inducteries, Ltd. Oleylamine was obtained from Tokyo Chemical Industry Co., Ltd. Mylar (thickness: 10 μm) was used as polymer thin film in small-angle XRD and SQUID measurements.

2. Apparatus. ^{1}H NMR data were measured by a JEOL AL-300 (300 MHz). ^{1}H NMR chemical shifts were determined by using tetramethylsilane (TMS) as an internal standard. Elemental analyses were performed with a Perkin-Elmer 2400II CHNS/O. XRD spectra were characterized by a Bruker AXS. MIP-MS were recorded on a HITACHI P-6000. High-resolution images of the EuS nanocubes were obtained with a Hitachi JEM-3100FEF TEM equipped with a tilting device (±60 degrees) and operated at 300 kV. SAXS measurements were carried out using a rotating anode X-ray generator (UltraX18, Rigaku), in which monochromatic X-ray of 1.54 Å in wavelength was focused through a Confocal Max-Flux mirror (Osmic). The diffraction images were collected using an X-ray image intensifier CCD detector (HAMAMATSU,

(11) (a) Regulacio, M. D.; Tomson, N.; Stoll, S. L. *Chem. Mater.* **2005**, *17*, 3114–3121. (b) Zhao, F.; Sun, H.; Gao, S.; Su, G. *J. Mater. Chem.* **2005**, *15*, 4209–4214. (c) Regulacio, M. D.; Bussmann, K.; Lewis, B.; Stoll, S. L. *J. Am. Chem. Soc.* **2006**, *128*, 11173–11179. (d) Zhao, F.; Sun, H.-L.; Su, G.; Gao, S. *Small* **2006**, *2*, 244–248. (e) Huxter, V. M.; Mikovic, T.; Nair, P. S.; Scholes, G. D. *Adv. Mater.* **2008**, *20*, 2439–2443. (f) Regulacio, M. D.; Kar, S.; Zuniga, E.; Wang, G.; Dollahon, N. R.; Yee, G. T.; Stoll, S. L. *Chem. Mater.* **2008**, *20*, 3368–3376. (g) Pereira, A. S.; Rauwel, R; Reis, M. S.; Silva, N. J. O; Barros-Timmons, A.; Trindade, T. *J. Mater. Chem.* **2008**, *18*, 4572–4578.

(12) (a) Xavier, R. M.; Fac. Sci., O. *Phys. Lett. A* **1967**, *25*, 244. (b) Thompson, W. A.; Penney, T.; Holtzberg, F.; Kirkpatrick, S. *Proc. Int. Conf. Phys. Semicond., 11th* **1972**, 2 1255.

(13) (a) Sun, S.; Murray, C. B.; Weller, D.; Folks, L.; Moser, A. *Science* **2000**, *287*, 1989–1992. (b) Shevchenko, E. V.; Talapin, D. V.; Schnablegger, H.; Kornowski, A.; Festin, R.; Svedlindh, P.; Haase, M.; Weller, H. *J. Am. Chem. Soc.* **2003**, *125*, 9090–9101. (c) Dumestre, F.; Chaudret, B.; Amiens, C.; Renaud, P.; Fejes, P. *Science* **2004**, *303*, 821–823. (d) Farrell, D.; Ding, Y.; Majetich, S. A.; Sanchez-Hanke, C.; Kao, C. C. *J. Appl. Phys.* **2004**, *95*, 6636–6638. (e) Nunes, W. C.; Cebollada, F.; Knobel, M.; Zanchet, D. *J. Appl. Phys.* **2006**, *99*, 08N705. (f) Sachan, M.; Walrath, N. D.; Majetich, S. A.; Krycka, K.; Kao, C. C. *J. Appl. Phys.* **2006**, *99*, 08C302. (g) Lisieki, I.; Parker, D.; Salzemann, C.; Pleni, M. P. *Chem. Matt.* **2007**, *19*, 4030–4036. (h) Parker, D.; Lisieki, I.; Salzemann, C.; Pleni, M. P. *J. Phys. Chem. C* **2007**, *111*, 12632–12638.

(14) Snoeck, E.; Gatel, C.; Lacroix, L. M.; Blon, T.; Lachaize, S.; Carrey, J.; Respaud, M.; Chaudret, B. *Nano Lett.* **2008**, *8*, 4293–4298.

(15) (a) Murray, C. B; Kagan, C. R.; Bawendi, M. G. *Science* **1995**, *270*, 1335–1338. (b) Kagan, C. R.; Murray, C. B.; Nirmal, M.; Bawendi, M. G. *Phys. Rev. Lett.* **1996**, *76*, 1517–1520. (c) Pileni, M. P. *Langmuir* **1997**, *13*, 3266–3276. (d) Talapin, D. V.; Shevchenko, E. V.; Kornowski, A.; Gaponik, N.; Haase, M.; Rogach, A. L.; Weller, H. *Adv. Mater.* **2001**, *13*, 1868–1871. (e) Talapin, D. V.; Murray, C. B. *Science* **2005**, *310*, 86–89. (f) Urban, J. J.; Talapin, D. V.; Shevchenko, E. V.; Murray, C. B. *J. Am. Chem. Soc.* **2006**, *128*, 3248–3255.

(16) Urban, J. J.; Talapin, D. V.; Shevchenko, E. V.; Kagan, C. R.; Murray, C. B. *Nat. Mater.* **2007**, *6*, 115–121.

V7739P/C-4880-50). The distance between sample and detector was adjusted to 750 mm. The magnetic measurements were carried out using a Quantum Design MPMS SQUID system (superconducting quantum interference devices magnetometer).

3. Synthesis of Tetraphenylphosphonum Tetrakis(diethyldithiocarbamate) Europium(III) ($(PPh_4)[Eu(S_2CNEt_2)_4]$). A solution of $(Na(S_2CNEt_2)\cdot 3H_2O)$ (14 g) in 30 mL of methanol was added to $EuCl_3\cdot 6H_2O$ (5.6 g) dissolved in 30 mL of methanol while stirring and reacted for 3 h. After the reaction mixture was filtered, a solution of $BrPPh_4$ (6.4 g) in 30 mL of methanol was added to the filtrated solution and stirred for 9 h. The resulting precipitate was separated by filtration and washed 2 times with ethanol. Yield: 30%. FT-IR spectrum (KBr): 1485−1482 (C−N) cm^{-1}, 1442 (P-Phenyl) cm^{-1}, 1007 (C−S) cm^{-1}. ^1H NMR spectrum (CD_3CN): 7.91 (4H, t, $J = 6.3$ Hz, $[Eu(S_2CNEt_2)_4]$ $(P(C_6\underline{H}_5)_4(p))$, δ7.70 (16H, m, $[Eu(S_2CNEt_2)_4]$ $(P(C_6\underline{H}_5)_4(o, m))$, δ3.17(8H, q, $J = 7$ Hz, $[Eu(S_2CNC\underline{H}_2CH_3)_4]$ (PPh_4)). δ1.61 (12H, q, $J = 7$ Hz, $[Eu(S_2CNCH_2C\underline{H}_3)_4]$ (PPh_4)). Anal. Calcd for $C_{44}H_{60}EuN_4PS_8$: C, 48.33; H, 5.53; N, 5.13%. Found: C, 48.31, H, 5.46, N, 5.13%.

4. Synthesis of Cube-Shaped EuS NCs: EuS NCs. Under N_2 atmosphere $(PPh_4)[Eu(S_2CNEt_2)_4]$ (0.5 g) was dissolved into oleylamine (4.5 g), and the mixture was heated at 180 °C and stirred for 20 min. After the reaction solvent was heated to 300 °C and stirred for 6 h, the purple liquid was centrifuged at 5000 rpm for 10 min. The precipitation was added to 8 mL of toluene and centrifuged at 13000 rpm for 15 min, and the clear purple liquid was obtained by elimination of the deposition.

5. Preparation of EuS NCs Superlattices Structures: SLSs. Obtained EuS NCs (3.1 mg) were dispersed in toluene (8 mL). TEM grids or polymer films were placed in the EuS NCs toluene solution (1 mL) in a vial with the substrate forming an angle of 30° with the surface of drying dispersion (Supporting Information Figure 1S). SLSs of 3D EuS NCs were prepared by slow evaporation (0.08 mL/h) of the toluene solution under room temperature. After complete drying of the toluene solution, the TEM grids or polymer films were dipped in methanol to remove an excess amount of oleylamine for TEM and small-angle XRD measurements and then dried in vacuum for 3 h. In order to prevent the partial oxidation on the EuS NCs surface as has been reported by Zhao et al[11b,d] prepared EuS assembly and powders were preserved under nitrogen atmosphere.

Results and Discussion

Preparation of EuS Nanocrystals. The cube-shaped EuS NCs were prepared by the thermal reduction of the single source precursor $[Eu(S_2CNEt_2)_4]$ under controlled reaction times and temperatures, 300 °C for 6 h. XRD confirmed the formation of crystalline EuS NCs (Figure 2). Diffraction peaks 2θ of XRD measurement = 25.5, 29.8, 42.6, 50.6, 53.1, 62.1, and 70.5° were assigned (111), (200), (220), (222), (400), (420), and (422) of NaCl type EuS, respectively. The crystal size of EuS calculated using the Scherrer's equation from diffraction peak (200) was found to be 12 nm (Figure 2(a)). The EuS NCs (average size = 14 nm) showed clear lattice-fringe profiles in their TEM images (Supporting Information Figures S2(a) and S3(a)), as typically shown in the inset of Figure 3(a). We also succeed in preparing sphere-shaped NCs with different preparation conditions. They also exhibited a characteristic XRD profile similar to that of Figure 2 as mentioned in the Supporting Information.

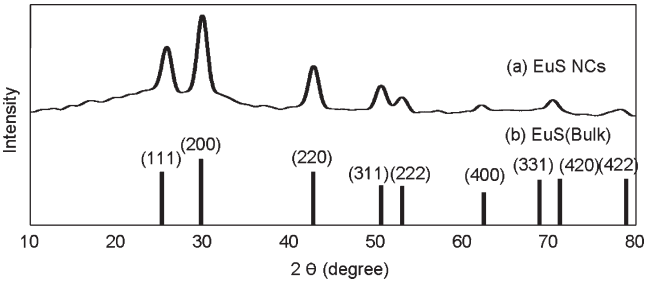

Figure 2. XRD profiles of (a) cube-shaped EuS NCs and (b) ASTM data of EuS (bulk).

The cube-shaped EuS NCs frequently showed formation of aggregated structures on the TEM girds substrates as typically shown in Figure 3(b). We also found that there are several types of NCs with different image-tones, which indicate existence of superimposed structures of the cubic EuS NCs. The NCs seem to be stacked for more than four layers in the case of Figure 3(b). Figure 3(c) was obtained with the tilting angle of −60° and is indicating a single SLS particle composed of EuS NCs $7 \times 8 \times 4$ NCs-aggregation structure. Figure 3(d),(e) was obtained by electron transmission tomographic analysis performed on commercially available software. Fine angular-dependent TEM images are provided in a movie file given in the Supporting Information. Since the sample of Figure 3 was prepared simply by casting the solution of EuS-NCs in toluene onto a TEM grid substrate, we concluded that the presented EuS-NCs spontaneously form the simple cubic SLSs with self-assemble arrangements. The SLSs size is dominated by concentration of EuS NCs in toluene and evaporation conditions. We also observed SLSs of various sizes in the TEM measurements; some of them are given in the Supporting Information Figure S4.

Characterization of the SLSs Assembled with EuS NCs. We attempted to prepare larger SLSs by the slow-evaporation procedure onto the TEM grid substrates and transparent polymer films. Figure 4 represents typical TEM images of SLSs obtained by the slow-evaporation procedure with EuS NCs ((a) and (b)). The EuS NCs formed large simple cubic SLSs with characteristic facets with orthogonal structures in the range of micrometer scale. The facets of the superstructure are characterized with (100) and (010) of the cubic SLSs. The characteristic 2D fast Fourier transform (FFT) image of the SLSs is shown in the insets of Figure 4(b), and the spots are assigned to (100) ($d_{100} = 17.0$ nm) and (110) ($d_{110} = 12.1$ nm). The FFT images clearly indicated the long-range ordering of these SLSs in the scale of 0.25 μm^2 for EuS NCs SLS. The center-to-center distance of the NCs based on the Fitzmaurice's calculation corresponds to $d_{100} = 17.0$ nm for SLS of EuS NCs.[17] From these 2D FFT images, the lattice constant of (100) was assigned to center-to-center distance (17 nm) of EuS NCs. The face-to-face distance between EuS NCs was estimated to be about 3 nm. On the other hand, length of oleylamine was estimated to be about 2.3 nm by DFT calculation. From these estimations, we consider

(17) Korgel, B. A.; Fullam, S.; Connolly, S.; Fitzmaurice, D. *J. Phys. Chem. B* **1998**, *102*, 8379–8388.

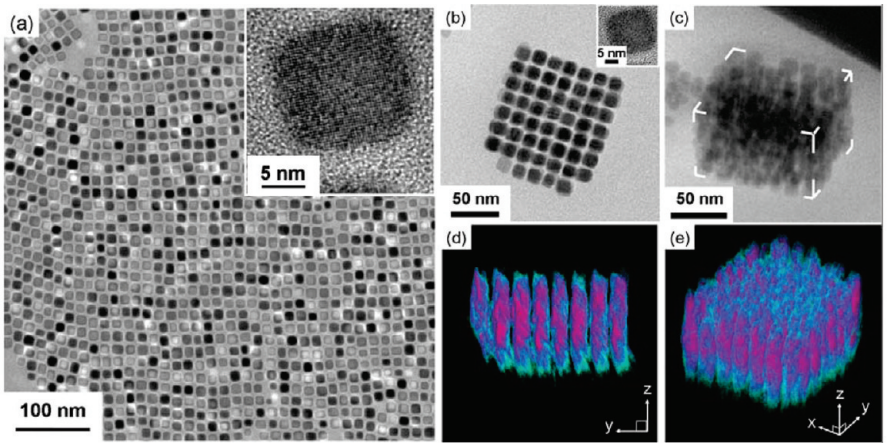

Figure 3. TEM images of cube-shaped EuS NCs observed by rotating the TEM grid at (a), (b) 0°, and (c) 60°. (d) and (e) Reconstruction 3D images of transmission electron tomography analysis of EuS NCs SLSs.

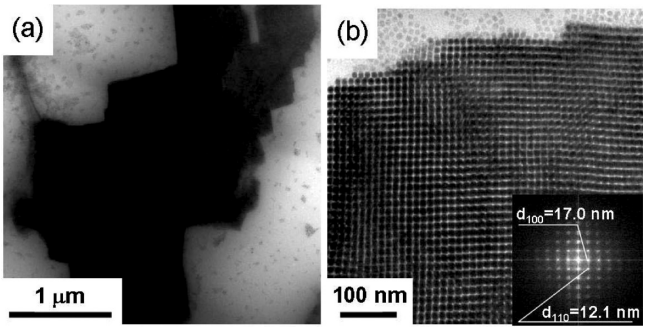

Figure 4. TEM images of SLSs assembled with (a) (b) EuS NCs. The fast Fourier transform (FFT) in the insets in (b) reveal simple cubic structure.

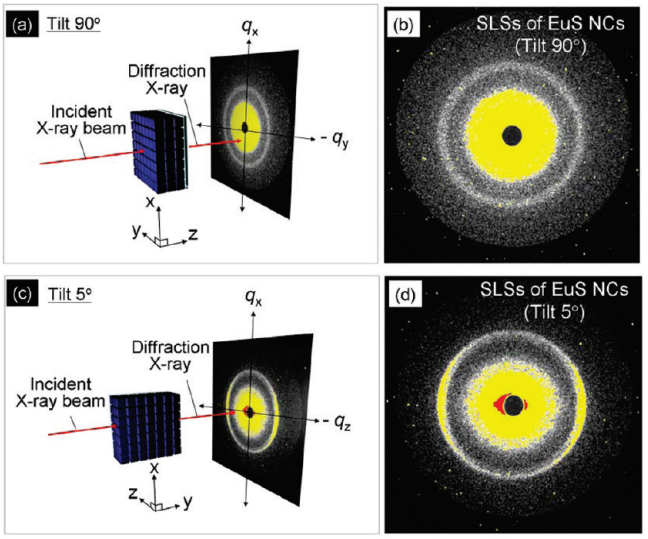

Figure 5. Schematic of the small angle XRD configuration: incident X-ray beam, sample tilted at (a) 90° and (c) 5°, diffraction X-ray beam, and CCD detector. Small angle XRD image of SLSs assembled with (b) EuS NCs on polymer films tilted at 90° and SLSs assembled with (d) EuS NCs on polymer films tilted at 5°.

that oleylamines might align in the bilayer manner between the EuS NCs with certain interdigitation.

In order to characterize 3D long-range ordering of EuS NCs, we measured small-angle XRD of SLSs of EuS NCs formed on polymer films, as shown in Figure 5. In the case of X-ray irradiation measurement with tilt angle of 90° as

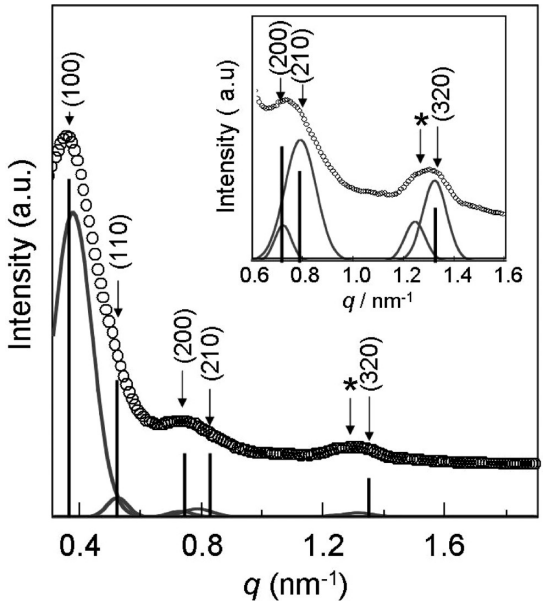

Figure 6. Small-angle XRD profiles of SLSs assembled with EuS NCs on polymer films tilted at 90°.

illustrated in Figure 5(a), we observed isotropic-ring diffraction pattern as shown in Figure 5(b). These results indicate 2D in-plane ordering of EuS NCs on the substrate surface. When EuS-NCs assembling on polymer films tilted at 5° were irradiated as illustrated in Figure 5(c), small-angle XRD intensities of q_z-direction were stronger than those of q_x-direction. These results mean that stacking structures of EuS NCs are constructed of not only 2D ordering but also 3D arrangements on the polymer thin films.

The small-angle XRD profiles of SLSs of EuS NCs on polymer films tilted 90° are shown in Figure 6. The diffraction peak position of q values are given by eq 1

$$q = 4\pi \sin \theta/\lambda \quad (1)$$

where θ and λ are the diffraction angle and 0.154 nm for the Cu−Kα line, respectively. There are some characteristic diffraction peaks which were assigned to the simple cubic SLSs as summarized in Table 1. Figure 6 also represents the results of fitting calculation for the diffraction profiles

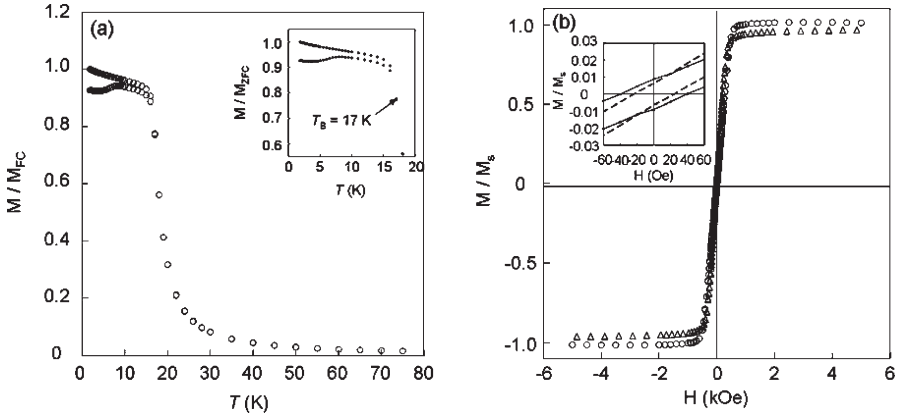

Figure 7. (a) FC and ZFC magnetization versus temperature curves, normalized to M_{FC} at 1.8 K of SLSs assembled with EuS NCs. (b) Magnetization versus field curves at 1.8 K, normalized to *M*s of SLSs (circle and solid line) and powders (triangle and dashed line) composed of EuS NCs.

Table 1. Peaks Position from Small Angle XRD Pattern of SLSs Assembled with EuS NCs on Polymer Film

compound	*hkl*	q (nm^{-1})	exp. q_{hkl}/q_{100}	cal. q_{hkl}/q_{100}
SLSs of EuS NCs	(100)	0.36	1.00	1.00
	(110)	0.51	1.42	1.41
	(200)	0.71	1.97	2.00
	(210)	0.78	2.16	2.24
	(320)	1.32	3.66	3.61

Table 2. Magnetic Properties of SLSs and Powders Composed of EuS NCs

compounds	blocking temperature, T_B (K)	coercive fields, H_C (Oe)
SLSs of EuS NCs	17.0	40
powder of EuS NCs	10.0	21

with Gauss's Functions. The diffraction peaks marked with an asterisk were attributed to the organized structure of oleylamine, which seems to cover the surface of the NCs (Supporting Information Figure S8). In Table 1, we also summarized a ratio of experimental q values against q_{100} for SLSs of EuS NCs (exp. q_{hkl}/q_{100}) and their calculated values for the cubic SLSs (cal. q_{hkl}/q_{100}) in Table 1. The observed q_{hkl}/q_{100} values in the SLSs agreed well with expected ones, supporting formation of simple cubic SLSs, respectively. Values of d_{100} evaluated from the XRD measurements were found to be 17.4 nm, which were again in good agreement with d_{100} of NCs from the 2D-FFT of the TEM images. The peak positions of XRD profiles tilted at 5° also agreed with those of tilted 90° (Supporting Information Figure S11). These small-angle XRD analyses indicate 3D arrangements of EuS NCs on polymer films in cubic superstructure. The SLSs composed of sphere-shaped EuS NCs can also be prepared on the polymer thin films as also presented in the Supporting Information.

Magnetic Property of the SLSs Composed of EuS NCs on Polymer Films. Magnetic properties of SLSs (see Table 2) assembled with EuS NCs on polymer films and powders were performed using SQUID measurements. The temperature dependence of the magnetic susceptibilities of EuS SLSs and powders of EuS NCs are shown in Figure 7 (a),(b). We found that the SLSs and powders of EuS NCs showed ferromagnetic behaviors. The blocking temperature (T_B), coercive fields (H_C), and magnetic remnant divided into magnetic saturation (M_R/M_S) of EuS SLSs were estimated to 17 K, 40 Oe, and 0.008, respectively. In contrast, these of powders samples of EuS NCs were found to be 10 K, 21 Oe, and 0.006, respectively (Supporting Information Figure S13(a)). The T_B and H_C of the SLSs of EuS NCs are two times larger than those of EuS NCs powder. In the case of magnetic NCs assembling, T_B and H_c are strongly dependent on shapes and arrangement condition of NCs.[13,18−22] Chaudret et al. have reported that highly ordered assembling of cube-shaped magnetic NCs indicated strong ferromagnetic dipole interaction between NCs.[13] We considered that the larger T_B and *H*c of SLSs assembled with EuS NCs might be due to strong magnetic dipole interaction between NCs in SLSs.

We observed unique magnetic properties of SLSs assembled with EuS NCs. That is, the blocking temperature and coercive fields of the SLSs were markedly higher than those of EuS NCs powders. These results indicated that magnetic properties of SLSs composed of EuS NCs are strongly depended on size, shape, and arrangement condition of NCs. Highly ordered assembling formation of EuS NCs could be exhibited enhanced magnetic properties by ferromagnetic dipole interaction between NCs.

Conclusion

In this study, we successfully observed the magnetic properties of the 3D assemblies of cube-shaped EuS NCs on polymer films. The blocking temperature and coercive fields of SLS of cube-shaped EuS NCs on the polymer films were twice larger than those of EuS NCs powders. The enhanced magnetic properties of SLSs assembled with EuS NCs are attributed to magnetic interaction between EuS NCs in SLSs. The SLSs composed of magnetic semiconductor EuS NCs are expected to be useful in applications such as novel magnetic-opto devices.

(18) Chudnovsky, E. M.; Serota, R. A. *J. Phys. C: Solid State Phys.* **1983**, *16*, 4181–4190.
(19) Chudnovsky, E. M. *J. Appl. Phys.* **1988**, *64*, 5770–5775.
(20) Chudnovsky, E. M. *J. Magn. Magn. Mater.* **1989**, *79*, 127–130.
(21) Filippi, J.; Amaral, V. S.; Barbara, B. *Phys. Rev. B.* **1991**, *44*, 2842–2845.
(22) Thomas, L.; Tuaillon, J.; Perez, J. P.; Dupuis, V.; Perez, A.; Barbara, B. *J. Magn. Magn. Mater.* **1995**, *140*, 437–438.

Acknowledgment. We thank for Ms. S. Fujita, Ms. R. Nakashima, Ms C. Goto, and Mr. M. Fujiwara in NAIST for their contribution on TEM observation and MIP-MS measurements. This work was partly supported by Grants-in-Aid for Scientific Research on Innovative Areas of Emergent chemistry of nano-scale molecular systems (2008-2012) from the Ministry of Education, Culture, Sports, Science and Tech (MEXT), Japan.

Supporting Information Available: Preparation of sphere-shaped EuS NCs, TEM images, movie file of electron transmission tomographic analysis of cube-shaped EuS NCs in WMV format, small-angle XRD data of oleylamine and SLSs assembled with sphere-shaped EuS NCs, and FC and ZFC magnetization versus temperature curves of SLSs and powder composed of cube and sphere-shaped EuS NCs. This material is available free of charge via the Internet at http://pubs.acs.org.